Identification problems and analysis of the limit current in fuel cells

Paolo Costa, Barbara Bosio *

Department of Civil, Environmental and Architectural Engineering, University of Genoa, Via Opera Pia 15, 16145 Genoa, Italy

ARTICLE INFO

ABSTRACT

This paper presents our analysis of the mass transfer phenomena in fuel cells. Our attention was specifically focused on the parameter identification problems (briefly identification problems) related to the interpretation of the experimental data on the limit current.

Two factors work together to make the interpretation of the limit current data difficult: the presence of two interacting electrodes (electrode coupling phenomena) and the flow rate changes along each electrode. The first effect can be well defined and understood by studying reagent-poor inlet flow rates to the electrodes; the second effect can be analysed by superimposition. In this analysis, the asymptotic solutions for complete decoupling conditions, that are complete anodic (or cathodic) mass transfer control, have been shown to be very useful reference tools.

© 2008 Elsevier B.V. All rights reserved.

1. Introduction

Today fuel cells are in a critical development stage, which can be facilitated with a work aimed at investigating basic phenomena more deeply as well as improving technologies and processes optimising performance, lifetime and costs.

In this scenario, a careful study of the mass transfer resistances can be interesting because operation under limiting-diffusion conditions can strongly penalise fuel cell functioning.

Usually studies focused on the improvement of fuel cell performance take account of the effects of the mass transfer resistances in terms of the concentration polarisation, the fuel utilisation factor or the limit current [1–3], nevertheless the subject is not usually approached from the point of view of experimental data interpretation. In this paper such an approach will be discussed.

Limit current experimental data, although relatively rare, are the most specific and direct way to characterise the mass transfer resistances of a cell, because, by definition, the limit currents are completely controlled by these resistances, while they are completely independent of the intrinsic electrochemical kinetics.

Mass transfer resistances, however, cannot be automatically and directly determined by limit current data without using some interpretative procedure. In fact, two factors work together to make the problem of mass transfer identification difficult: the electrode coupling phenomena and the flow rate changes along each electrode.

The first effect corresponds to a mixed mass transfer control; it acts when only a portion of the cell is controlled by anodic mass transfer phenomena (e.g. H_2 is the limiting reactant) while the remaining portion is controlled by cathodic ones (e.g. oxidant is the limiting reactant) [4]. This effect can be isolated from the second by studying reagent-poor inlet flow rates to the electrodes and determining the fraction of the cell surface which undergoes anodic (or cathodic) mass transfer control under such simple conditions.

The second effect depends on the non-linear relationship between the utilisation factor and the reagent concentration in reagent-rich systems: as already shown in our previous works [5,6] a superficial analysis of the concentration field effects can lead to significant errors in the estimation of the mass transfer coefficients.

In the following sections these two effects and their superimposition will be discussed in order to provide correct data interpretation.

The work refers in particular to molten carbonate fuel cell (MCFC) technology, but its matter is valid for each kind of fuel cells.

2. The reference case

Reference has been made to a cross-flow fuel cell (in particular an MCFC, which is a molten carbonate fuel cell) of a typical industrial laboratory scale (with a rectangular $L_x \times L_y$ shape, about $0.1 \, m \times 0.1 \, m$) [6]. Such laboratory devices can be considered substantially isothermal and isobaric, while their flow field can be schematised as a cross-coupling of two plug-flow systems, namely an anodic one flowing from left to right and a cathodic one flowing upwards.

* Corresponding author. Tel.: +39 010 353 6505; fax: +39 010 353 2589.
E-mail address: barbara.bosio@unige.it (B. Bosio).

Moreover, for a first, simplified approach, reagent-poor solutions and invariant volumetric flow rates can be assumed for the anodic (uniform q_A) and the cathodic (uniform q_C) sides, respectively. Finally, explicit reference has been made to the limit current condition, which has been assumed over the entire cell plane, so that the local kinetics are everywhere controlled by transport phenomena and, more precisely, by which of the two reactant diffusive transport mechanisms is slower, the anodic or the cathodic:

$$r = \frac{J}{nF} = \min(k_{cLA}C_{LA}, k_{cLC}C_{LC}) \tag{1}$$

For instance, in an MCFC, where the reactions

$$H_2 + CO_3{}^{2-} \rightarrow H_2O + CO_2 + 2e^- \quad \text{(at the anode)}$$

$$CO_2 + \tfrac{1}{2}O_2 + 2e^- \rightarrow CO_3{}^{2-} \quad \text{(at the cathode)}$$
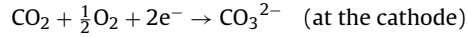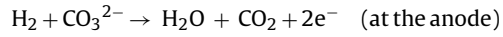
occur (neglecting the possibility of direct oxidation of CO or hydrocarbons), the anodic reactant is hydrogen (LA = H_2) and the cathodic limiting reactant is normally carbon dioxide (LC = CO_2), while the second cathodic reactant, oxygen, is present in excess and does not show any limiting effect.

In such simple circumstances the local mass balances of the anodic reagent LA and the cathodic reagent LC can be written, respectively as

$$q_A\frac{\partial C_{LA}}{\partial X} = -\min(k_{cLA}C_{LA}, k_{cLC}C_{LC})L_y, \quad 0 < X < L_x,$$
$$X = 0; \ C_{LA} = C_{LAo} \tag{2}$$

and

$$q_C\frac{\partial C_{LC}}{\partial Y} = -\min(k_{cLA}C_{LA}, k_{cLC}C_{LC})L_x, \quad 0 < Y < L_y,$$
$$Y = 0; \ C_{LC} = C_{LCo} \tag{3}$$

or in the compact forms

$$\zeta_A = k_{cLa}C_{LA}, \quad x = Xk_{cLA}\frac{L_y}{q_A}, \quad x_t = L_xk_{cLA}\frac{L_y}{q_A};$$
$$\zeta_C = k_{cLC}C_{LC} \quad y = Yk_{cLC}\frac{L_x}{q_C}, \quad y_t = L_yk_{cLC}\frac{L_x}{q_C} \tag{4}$$

$$\frac{\partial \zeta_A}{\partial x} = -\min(\zeta_A, \zeta_C), \quad 0 < x < x_t = k_{c\,LA}L_x\frac{L_y}{q_A}, \quad x = 0; \ \zeta_A = \zeta_{Ao} \tag{5}$$

$$\frac{\partial \zeta_C}{\partial y} = -\min(\zeta_A, \zeta_C), \quad 0 < y < y_t = k_{cLC}L_y\frac{L_x}{q_C},$$
$$y = 0; \ \zeta_C = \zeta_{Co} = \Psi\zeta_{Ao} \tag{6}$$

introducing the parameter $\Psi = \zeta_{Co}/\zeta_{Ao}$.

3. Simple and mixed control conditions

According to Eqs. (5) and (6), the plane of the cell can be divided into two zones (Fig. 1): one, where $\zeta_A < \zeta_C$, which is controlled by the anodic mass transfer phenomena, and one, where $\zeta_C < \zeta_A$, which is controlled by the cathodic transfer phenomena. The boundary between these two zones is obviously defined by the condition $\zeta_A = \zeta_C$ and, then, described by the straight line equation (see Appendix A):

$$y = \Psi(1 + x) - 1, \quad \Psi = \frac{\zeta_{Co}}{\zeta_{Ao}} = \frac{k_{cLC}C_{LCo}}{k_{cLA}C_{LAo}} \tag{7}$$

or, in terms of the intercept of the boundary on the left margin of the cell:

$$y = y_{x=0} + \Psi x, \quad y_{x=0} = \Psi - 1 \tag{8}$$

The comparisons of the $y_{x=0}$ value given by the second Eq. in (8) and the y_t value given by the second Eq. in (6) and of the y value given by the first Eq. in (7) and the x_t value given by the second Eq. in (5) show that the cell can undergo three different kinds of current limitations:
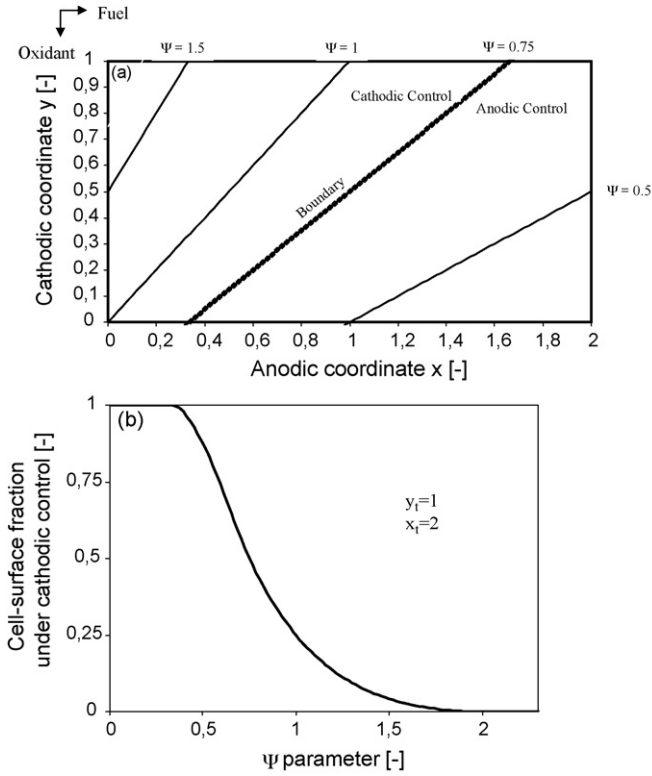
Fig. 1. Cross-flow fuel cell under limit current conditions. (a) Changing of the boundary position for different values of parameter Ψ. (b) Cell-surface fraction working under cathodic control conditions versus parameter Ψ (underlined as an example the boundary for $\Psi = 0.75$). For a cell with $y_t = 1$, $x_t = 2$, the complete anodic control requires $\Psi > 2$, while the complete cathodic control requires $\Psi < 1/3$. In intermediate conditions ($1/3 < \Psi < 2$), the cell works under mixed control.

- Simple anodic mass transfer control:

for $\Psi > 1 + y_t$ (9)

The boundary position is characterised by $y > y_t$ for $0 < x < x_t$: the boundary lies to the left of the upper-left edge of the cell and does not cross it, so that $\zeta_A < \zeta_C$ and the anodic mass transfer controls each point of the cell. In such case the boundary can be called "external".

- Simple cathodic mass transfer control:

for $\Psi < (1 + x_t)^{-1}$ (10)

The "external" boundary position is now characterised by $y < 0$ for $0 < x < x_t$: the boundary lies to the right of the lower-right edge of the cell and again does not cross it. In this case $\zeta_C < \zeta_A$ and the cathodic mass transfer controls each point of the cell.

- Mixed mass transfer control:

for $(1 + x_t)^{-1} < \Psi < 1 + y_t$ (11)

In this case the boundary crosses really the cell and divides it into two parts, the upper under anodic control and the lower under cathodic control. Under such conditions, the fraction of the cell surface working under cathodic control increases from zero to unity with the decrease in parameter Ψ in the range of Eq. (11). An example of this trend is given in Fig. 1, which refers to a cell "shape" $x_t = 1$, $y_t = 2$ and a mixed control range $1/3 < \Psi < 2$.

Using Eq. (7) the value of $\zeta_b(x)$ acting on the boundary can also be obtained (see Appendix A). An example is shown in Fig. 2.
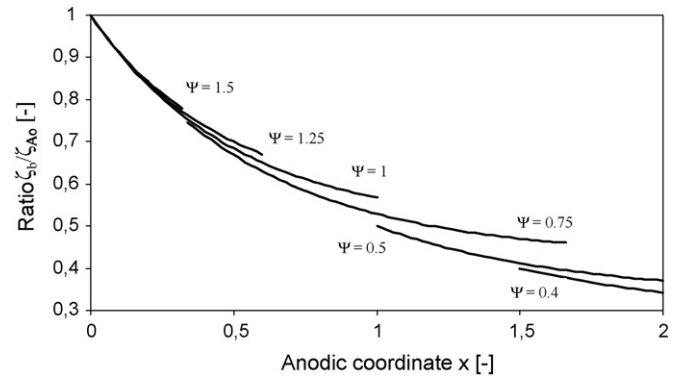

Fig. 2. Cross-flow fuel cell under limit current conditions: an example of the trend of the ratio ζ_b/ζ_{Ao} along the boundary between the anodically and cathodically controlled zones, for $y_t = 1$, $x_t = 2$ and different values of Ψ ($\Psi = 1.5$ for $0 < x < 0.33$; $\Psi = 1.25$ for $0 < x < 0.6$; $\Psi = 1$ for $0 < x < 1$; $\Psi = 0.75$ for $0.33 < x < 1.66$; $\Psi = 0.5$ for $1 < x < 2$; $\Psi = 0.4$ for $1.5 < x < 2$). When $\Psi > 2$ (complete anodic control) and $\Psi < 1/3$ (complete cathodic control) the boundary does not cross the cell.

4. The limit performance of the cell

The performance of a cell working under a simple mass transfer control can be straightforwardly predicted: for instance, the anodic utilisation factor for a cell under simple anodic control is [4]

$$u_A = u_{LA} = 1 - \exp(-x_t), \quad \Psi > 1 + y_t \tag{12}$$

Obviously a similar expression holds for the cathodic utilisation under simple cathodic control. In such circumstances the anodic utilisation factor is

$$u_A = u_{LC} \frac{\Psi x_t}{y_t}, \qquad u_{LC} = 1 - \exp(-y_t), \quad \Psi < (1 + x_t)^{-1} \tag{13}$$

Under mixed control conditions, the anodic composition lies within the limits of Eqs. (12) and (13) (see Appendix A). An example of the results obtained is given in Fig. 3, where the anodic utilisation is reported as a function of the parameter Ψ and the limit trends for complete anodic control, Eq. (12), and complete cathodic control, Eq. (13), are shown as well.

In Fig. 3 complete anodic or cathodic control corresponds to $\Psi > 2$ and $\Psi < 1/3$, respectively, but it is evident that the asymptotic solutions (12) and (13) can be considered sufficiently accurate over wider ranges of values, namely $\Psi > 1$ and $\Psi < 0.6$. Moreover, for many purposes the validity of the asymptotic behaviour can be extended to the intersection point.

$$\Psi^* = \frac{y_t[1 - \exp(-x_t)]}{x_t[1 - \exp(-y_t)]} \tag{14}$$
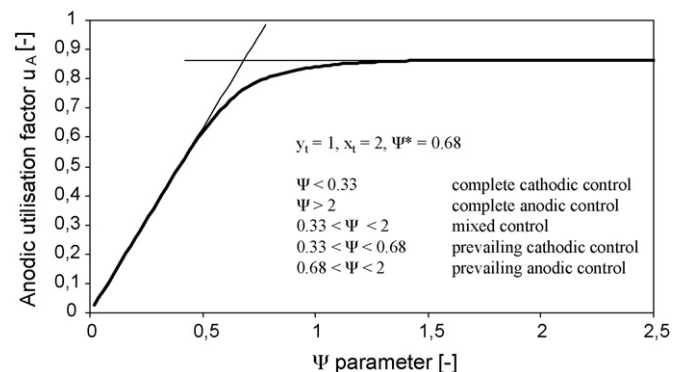

Fig. 3. Cross-flow fuel cell under limit current conditions: an example of the trend of the anodic utilisation factor for $y_t = 1$, $x_t = 2$ and for different values of Ψ.

with a maximum error, just at the intersection point, of the order of 10%. In such a way, the mixed control zone can be divided in two parts:

$$\Psi^* < \Psi < 1 + y_t, \quad u_A \approx u_{LA} \quad \text{(prevailing anodic control)};$$

$$(1 + x_t)^{-1} < \Psi < \Psi^*, \quad u_A \approx u_{LC} \Psi \frac{x_t}{y_t} \quad \text{(prevailing cathodic control)}$$
(15)

Another way of arranging the above results is to relate them to a cell working under constant inlet conditions in terms of reactant concentration for one electrode (e.g. the cathode, constant C_{LCo}) and variable inlet conditions for the other (anode, variable C_{LAo}).

As the cell current is proportional to the anodic utilisation and the anodic reagent inlet rate

$$I = nF q_A C_{LAo} u_A$$
(16)

the limit current of the cell can be obtained by Eq. (16), in which the limit utilisation is expressed by equations such as (A16), (A17) or by the approximations (15), (12), (13). In particular, for constant q_A, q_C, C_{LCo} and variable C_{LAo}, the limit current will be proportional to u_A and the inlet ratio $q_A C_{LAo}/q_C C_{LCo} = \text{const.}/\Psi$, so that the asymptotic trends of the cell will be

$$\Psi > \Psi^*, \quad I \approx I_A = \frac{\text{const.}}{\Psi}; \qquad \Psi < \Psi^*, \quad I \approx I_C = \text{const.}$$
(17)

as shown in Fig. 4.

The relevant point is that experimental findings are characterised by this kind of trend in terms of limit current and anodic composition, see Fig. 5. As the anodic inlet concentration is increased, the limit current increases too, initially: under these conditions there is complete, or at least prevailing, anodic control, in other words the two electrodes are completely decoupled and only the anode is significant. After a narrow mixed control range (significantly coupled electrodes), the limit current becomes constant, as it is controlled by the constant cathode: now the cell works under complete, or at least prevailing, cathodic control and the decoupling of the electrodes is again good, with only the cathode being significant [4].

The experimentally confirmed applicability of the discussed analytical approach to small-size cells puts in evidence its usefulness in terms of analysis and diagnostic aims.

Considering commercial cells of full area (usually about 1 m^2), the non-uniformity of the chemico-physical properties on the cell plane can be significant. In particular, the temperature, flow rate and transport coefficient distributions can affect the cell behaviour,
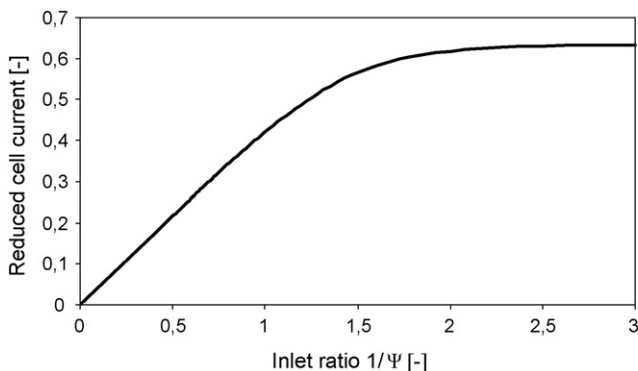

Fig. 4. Cross-flow fuel cell under limit current conditions: the cell current as a function of the anodic inlet under constant cathodic conditions. The cell current is reduced in respect to the complete conversion of the cathodic flow.
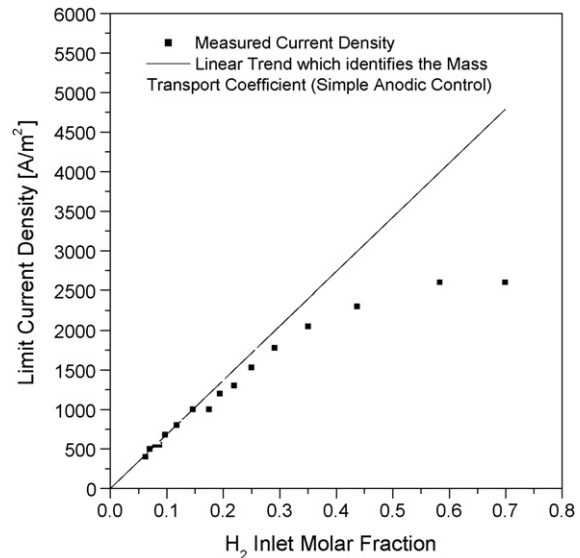

Fig. 5. Cross-flow fuel cell under limit current conditions: the experimental cell current as a function of the anodic inlet under constant cathodic conditions.

so that the predictable boundary position could need some corrections. On the other hand, it is interesting to observe that the boundary linearity is well confirmed for commercial MCFCs working under standard operating conditions. This fact has been verified by means of simulation with a detailed model [7].

5. Flow rate effects

As electrode reactions are not equimolar, the molar flow rates can undergo significant changes in flowing along the electrode paths. Under constant temperature and pressure the same changes affect the volumetric flow rates too. For instance, the anodic flow rate in an MCFC increases along the reaction path and so depends on the molar fraction of the hydrogen present [5]. In terms of volumetric flow rate and concentration the dependence is

$$q_A = q_{Ao} \frac{C + \nu_A C_{LAo}}{C + \nu_A C_{LA}}, \quad \nu_A = -\sum \frac{\nu_{Ai}}{\nu_{ALA}}$$
(18)

or, by using the definition of ζ_A in Eq. (4),

$$\frac{q_A}{q_{Ao}} = \frac{1 + f_A \zeta_{Ao}}{1 + f_A \zeta_A}, \quad f_A = \frac{\nu_A}{k_{cLA} C}$$
(19)

It is evident that, as $\nu_A = 1$ in MCFCs, for a dilute reactant ($C_{LA} \to 0$) the volumetric flow rate can be considered as a constant, while it tends to a 100% variation if pure hydrogen is fed.

Similarly, the volumetric flow rate at the cathode, where $\nu_c = -1.5$ in MCFCs, will decrease according to

$$\frac{q_C}{q_{Co}} = \frac{1 + f_C \zeta_{Co}}{1 + f_C \zeta_C}, \quad f_C = \frac{\nu_C}{k_{cLC} C} = \frac{-\sum \nu_{Ci}/\nu_{CLC}}{k_{cLC} C}$$
(20)

so that assuming now

$$x = X k_{cLA} \frac{L_y}{q_{Ao}}, \quad y = Y k_{cLC} \frac{L_x}{q_{Co}}$$
(21)

Eqs. (5) and (6) become

$$\frac{(\partial \zeta_A/\partial x)(1 + f_A \zeta_{Ao})}{(1 + f_A \zeta_A)^2} = -\min(\zeta_A, \zeta_C), \qquad x = 0, \quad \zeta_A = \zeta_{Ao}$$
(22)

$$\frac{(\partial \zeta_C/\partial y)(1 + f_C \zeta_{Co})}{(1 + f_C \zeta_C)^2} = -\min(\zeta_A, \zeta_C), \qquad y = 0, \quad \zeta_C = \zeta_{Co}$$
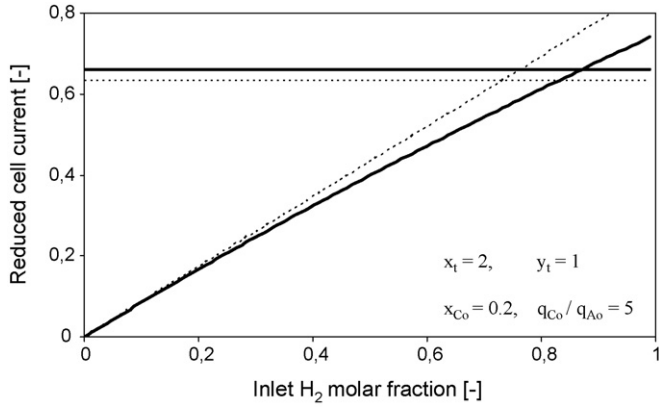(23)

Fig. 6. Cross-flow fuel cell under limit current conditions: an example of the effect of changing the flow rate on the asymptotic solutions for the cell. The approximate asymptotic solutions, calculated assuming uniform flow rates along the electrodes (dotted lines), are compared to the correct ones (continuous lines).

The system (22), (23) can be reduced to the form (5), (6) when the differential substitutions

$$dx' = \frac{(1+f_A\zeta_A)^2}{1+f_A\zeta_{Ao}}\,dx, \qquad dy' = \frac{(1+f_C\zeta_C)^2}{(1+f_C\zeta_{Co})}\,dy \tag{24}$$

are introduced.

In such a way, most of the results of the previous section can be rewritten and extended to those cases, frequent in practice, where the hypothesis of uniform flow rates has to be rejected in a fairly accurate description. In particular, the anodic utilisation u_A or the cell current I can be calculated for any feed composition (z_{LAo}, z_{LCo}) when the transport coefficients (k_{cLA}, k_{cLB}) are known or, inversely, in an identification problem, a best fit for the transport coefficients can be performed from measured I data. When mixed mass-transfer conditions are controlling, however, the calculations are not immediate and the explicit solutions cannot be expressed in analytical form.

In particular, the asymptotic solutions (12) and (13) are substituted by implicit equations such as the following:

- Anodic asymptotic solution:

$$u_A = u_{LA}, \qquad \frac{I}{nF} = q_{Ao}C_{LAo}u_{LA}$$

with $x_t = -[z_{LAo}\nu_A u_{LA} + (1+z_{LAo}\nu_A)\ln(1-u_{LA})]$ (25)

- Cathodic asymptotic solution:

$$u_A = \frac{u_{LC}q_{Co}C_{LCo}}{q_{Ao}C_{LAo}}, \qquad \frac{I}{nF} = q_{Co}C_{LCo}u_{LC}$$

with $y_t = -[z_{LCo}\nu_C u_{LC} + (1+z_{LCo}\nu_C)\ln(1-u_{LC})]$ (26)

In such a case, if a cell is working under complete anodic control, the dependence of the limit current on the composition of the anodic feed is no longer a simple proportionality (see Fig. 4). On the contrary, significant non-linear effects are evident as the hydrogen content increases: an example is shown in Fig. 6, where the approximate asymptotic solutions, calculated assuming uniform flow rates along the electrodes (dotted lines), are compared with the correct ones (continuous lines). The example refers to a constant inlet composition at the cathode ($Z_{LCo} = 0.2$) and inlet flow rate ratio ($q_{Co}/q_{Ao} = 5$), the values being chosen with reference to a typical run of an laboratory MCFC [6].

6. Conclusion

In this paper a discussion of the parameter identification problems affecting a mass transport phenomena study has been presented in order to provide a guide to a correct analysis of the limit current in fuel cells. A particular reference to molten carbonate fuel cells has been done.

Analysing the behaviour of a laboratory fuel cell under limiting-diffusion conditions and uniform temperature, a boundary on the cell plane has been identified distinguishing the area under the anodic control and the area under the cathodic control and so underlining the possibility of a mixed control. This boundary has been demonstrated linear when the flow-rate variation along the cell is negligible.

In addition, a linear trend of the cell limit current versus reagent concentration has been shown when complete decoupling conditions, that are complete anodic (or cathodic) mass transfer control, are considered. Such asymptotic solutions have been demonstrated a useful reference tool, which can involve a maximum error of the order of 10% in case of mixed control.

By this way the interpretation of the limit-current data, which are the most specific and direct data to characterise the mass transfer resistances of a cell, has been shown complicated by two non-linearity effects: mixed control and flow rate effects.

The interpretation of such non-linearity effects has been discussed and shown to be difficult to interpret, as the two effects tend to obscure each other.

In the light of such considerations, detailed local studies and specific tests involving complete electrode phenomena decoupling and reagent-poor feeds are advisable for evaluating diffusion contributions. Using this approach it is possible to obtain a better analysis of the fuel cell's performance and, consequently, more effective performance-improvement policies can be set up.

Appendix A

A.1. The position of the boundary

The boundary is defined by the position $\zeta_A = \zeta_B = \zeta_b$. Moreover, starting from the point $(x, 0)$ and following the cathodic flow upward ($x = $ const.) through the anodic control zone to the boundary point (x, y_b), we have

$$\zeta_b = \zeta_{Bo} - \int_0^{y_b} \zeta_A\,dy \tag{A1}$$

and, by differentiation and incorporating Eq. (5) in the above Eq. (A1),

$$\frac{d\zeta_b}{dx_b} = -\int_0^{y_b}\frac{d\zeta_A}{dx}\,dy - \frac{\zeta_A dy_b}{dx_b} = \int_0^{y_b}d\zeta_A dy - \frac{\zeta_A dy_b}{dx_b} = \zeta_{Co} - \zeta_b$$
$$- \frac{\zeta_b dy_b}{dx_b} \tag{A2}$$

Similarly, starting from the point $(0, y)$ and following the anodic flow from left to right ($y = $ const.) into the cathodic control zone to the boundary point (x_b, y), we have

$$\frac{d\zeta_b}{dy_b} = \zeta_{Ao} - \zeta_b - \frac{\zeta_b dx_b}{dy_b} \tag{A3}$$

By combining Eqs. (A2) and (A3), it is possible to obtain the differential equation of the boundary line:

$$\frac{dy_b}{dx_b} = \frac{\zeta_{Co}}{\zeta_{Ao}} \tag{A4}$$

The boundary condition for Eq. (A4) can be obtained from Eq. (A1) written for $x = 0$:

$$x = 0, \quad y_b = y_{x=0}, \quad \zeta_{Ao} = \zeta_{Co} - \zeta_{Ao}y_{x=0} \tag{A5}$$

By putting

$$\Psi = \frac{\zeta_{Co}}{\zeta_{Ao}} \tag{A6}$$

Eqs. (A4) and (A5) can be rewritten

$$\frac{dy_b}{dx_b} = \Psi, \qquad x = 0, \quad y_b = y_{x=0} = \Psi - 1 \tag{A7}$$

so that, by integration, the boundary can be described by the straight line equation:

$$y_b = \Psi x_b + \Psi - 1 \tag{A8}$$

A.2. The degree of cathodic control

Starting from Eq. (8), elementary geometrical considerations make it possible to evaluate the fraction φ_c of the cell surface which is under cathodic control. For instance, under the condition $x_t > y_t$, we have (see Fig. 1)

$$\begin{aligned}
\varphi_c &= 0, \quad \text{for } \Psi > 1 + y_t \\
\varphi_c &= \frac{(y_t - \Psi + 1)^2}{2\Psi y_t x_t}, \quad \text{for } 1 < \Psi < (1 + y_t) \\
\varphi_c &= \frac{y_t - 2\Psi + 2}{2\Psi x_t}, \quad \text{for } (1 + y_t)(1 + x_t)^{-1} < \Psi < 1 \\
\varphi_c &= \frac{(\Psi x_t - 1 + \Psi)^2}{2\Psi y_t x_t}, \quad \text{for } (1 + x_t)^{-1} < \Psi < (1 + y_t)(1 + x_t)^{-1} \\
\varphi_c &= 1, \quad \text{for } \Psi < (1 + x_t)^{-1}
\end{aligned} \tag{A9}$$

A.3. The composition on the boundary

By combining the differential Eqs. (A2) and (A4) with the position (A6), the changing composition along the boundary can be described as

$$\frac{d\zeta_b}{dx_b} = \Psi\zeta_{Ao} - \zeta_b(1 - \Psi) \tag{A10}$$

The starting condition for Eq. (A10) can be

$$x_b = 0, \quad \zeta_b = \zeta_{Ao}, \quad 1 < \Psi < 1 + y_t \tag{A11}$$

or

$$x_b = \frac{1 - \Psi}{\Psi}, \qquad \zeta_b = \Psi \zeta_{Ao}, \quad (1 + x_t)^{-1} < \Psi < 1 \tag{A12}$$

according to whether the boundary starts on the left side or on the lower side of the cell.

The integration of the Eq. (A10) with the condition (A11) or (A12) gives, respectively:

$$\frac{\zeta_b}{\zeta_{Ao}} = \frac{\Psi + \exp[-(1 + \Psi)x_b]}{1 + \Psi}, \quad 1 < \Psi < 1 + y_t \tag{A13}$$

$$\frac{\zeta_b}{\zeta_{Ao}} = \frac{\Psi + \Psi^2 \exp[(1 - \Psi^2)/\Psi] \exp[-(1 + \Psi) x_b]}{1 + \Psi},$$

$$(1 + x_t)^{-1} < \Psi < 1 \tag{A14}$$

A.4. The performance of the cell in terms of utilisation

Under simple control conditions the anodic utilisation factor of the cell is well described by Eqs. (12) and (13), for complete anodic and cathodic controls, respectively. Under mixed control conditions, the anodic composition at a point on the right side, which is delimited by the boundary and where the anodic mass transfer is controlling, is

$$\zeta_A(x) = \zeta_{Ao} \exp(-x), \quad x_b < 0; \quad \zeta_A(x) = \zeta_b \exp(x_b - x), \quad x_b > 0 \tag{A15}$$

so that the mean outlet composition is

$$\zeta_{Am} = \zeta_{Ao}(1 - u_A) = \int_0^y \zeta_A(x_t) \, dy \tag{A16}$$

Substituting Eqs. (A13) or (A14) with ζ_b and making the integral in Eq. (A16), the following results can be obtained:

$$\begin{aligned}
1 - u_A &= \exp(-x), \quad \Psi > 1 + y_t \\
1 - u_A &= \frac{\exp(-x)\{\Psi^2 \exp[(y_t/\Psi) - 1 + 1/\Psi] - \exp(\Psi - 1 - y_t)\}}{(1 + \Psi)y_t}, \\
& \quad 1 < \Psi < 1 + y_t \\
1 - u_A &= \frac{\exp(-x)\{\Psi^2 \exp[(y_t/\Psi) - 1 + 1/\Psi] - \exp[(\Psi/1) - 1 - y_t)]\}}{(1 + \Psi)y_t}, \\
& \quad (1 + y_t)/(1 + x_t) < \Psi < 1 + y_t
\end{aligned} \tag{A17}$$

and so on, from elementary symmetry considerations, as Ψ decreases to $(1 + x_t)^{-1}$.

An example of the results obtained is given in Fig. 3.

References

[1] F. Zhao, A.V. Virkar, J. Power Sources 141 (2005) 79–95.
[2] M. Baranak, H. Atakul, J. Power Sources 172 (2007) 831–839.
[3] G.F. Naterer, C.D. Tokarz, J. Avsec, Int. J. Heat Mass Transf. 49 (2006) 2673–2683.
[4] E. Arato, B. Bosio, P. Costa, F. Parodi, J. Power Sources 102 (2001) 74–81.
[5] P. Costa, B. Bosio, J. Power Sources 172 (2007) 334–345.
[6] P. Costa, B. Bosio, J. Power Sources 172 (2007) 346–357.
[7] F. Parodi, B. Bosio, E. Arato, International Patent Application PCT/EP2005/000028, Publication N. WO 2006/072262 A1 (2006), pp. 1–48.